

**MECHANICS OF POWDER HYDRO CANNON  
FOR INCOMPRESSIBLE FLUID**

O.P. Petrenko, E.S. Geskin  
New Jersey Institute of Technology  
Newark, New Jersey, U.S.A.

A.N. Semko  
Donetsk National University,  
Donetsk, Ukraine

**ABSTRACT**

The impact-based formation of the high speed liquid projectiles (impulsive jets) is investigated numerically. The jet formation is determined by both waves generated in the liquid in the course of impact as well as the conversion of the projectile in the nozzle and barrel. Comparative contribution of each factor is important for design of the facilities for formation of the impulsive as well as continuous jets. In order to evaluate the effect of the wave formation on the fluid acceleration the relationship between the jet velocity and fluid compressibility was estimated. Two numerical techniques were used for their estimation. The first one involved determination of the jet velocity for expulsion of the incompressible liquid. The second one involved application of the existing model for estimation of the exit velocity at various values of the liquid compressibility. The results of the computations enabled us to evaluate the effect of the various factors, particularly fluid compressibility, on the process results

## 1. INTRODUCTION

The high speed liquid projectiles (impulsive waterjets) constitute a highly efficient technological tool. At the velocities of 1000-2000m/s these projectiles release hundreds of megawatts of power in the course of the interaction with a target. This power is comparable with the power released by a high explosive detonating on the target surface. However while the projectile released precisely directed negligible amount of energy, in most cases much larger amount of energy of explosion is spread in less organized fashion.. This constitutes an important technological and environmental advantage of the liquid impact and determines its potential applications in mining, construction, manufacturing, medicine, etc.

A variety of launchers for generation of these projectiles were suggested [1, 2]. One of such launchers termed a hydro cannon is depicted on Fig.1. Conceptually, the hydro cannon constitutes a cylindrical barrel with a converging nozzle and a cylindrical attachment at the end, termed collimator. Energy provided by the powder combustion, oxygen-hydrogen reaction, gas expansion, electrical discharge, mechanical impact, laser beam, magnetic field, etc accelerates a water projectile located in a barrel [1-6]. In a converging nozzle the kinetic energy of the projectile is redistributed. The front significantly accelerates while main body decelerates. As the result, at the exit of the collimator water can reach velocity of several km/s.

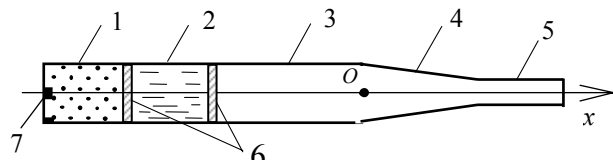


**Figure 1.** Schematic of Hydro cannon. 1-powder charge, 2-water load (slug), 3-barrel, 4-nozzle, 5-cylindrical attachment (collimator), 6-water load, 7-primer

The impacting high speed projectiles demolish brittle materials such as rocks or concrete. The metal deformation during the impact is similar to that during the explosive forming. This process similarly to the explosive forming requires only a single die. The second die is replaced by a liquid punch. This simplifies the forming facilities and reduces its cost. However, the high-energy liquid impact has unique features, which in many cases make it superior to other kinds of forming, including the explosive forming. The hydro cannon is a simple autonomous device, which can be readily integrated in a robotic arm. This enables us to move it across the workpiece surface, position at desired sites at a desired angle and impact a workpiece one or several times at controllable conditions. Several cannons can be used simultaneously.

Theoretical and experimental research has shown that among other hydro cannon designs, presented here, the powder hydro cannon has following advantages:

- design simplicity,
- small size and mass,
- large specific power due to a compact energy source,
- simplicity of generating high-speed water slugs with large diameter (up to 30-50mm), which carry immense specific energy and impulse,
- capability to generate relatively long water slugs,
- potential to significantly increase the effective standoff distance.

The force exerted on the workpiece in the course of the projectile impact is determined by the amount of the energy injected into water, the standoff distance and other process variables. All

these variables, and thus the exerted force, can be precisely controlled. Thus, at least in principle, precision control of forming operations regardless of the size and shape of the workpiece becomes possible and inexpensive. Because a desired site of the workpiece can be impacted several times it becomes possible to enhance material deformation, e.g. to pierce deep openings in a workpiece. Because the shape of a nozzle can vary in a wide range, the opening can have a desired geometry. Because the weight and size of the cannon can be significantly reduced, the desired opening can be generated by a portable device.

In the performed theoretical investigations of powder hydro cannon a one dimensional flow of ideal compressible fluid was used to represent the water stream. This flow was described by a system of equations of the non-stationary gas dynamics, which was numerically solved using Godunov method [7].

Current work describes general theory of powder hydro cannon for ideal incompressible fluid, which is mathematically reduced to a system of the ordinary differential equations. The numerical solutions of the constructed equations were used to evaluate the process potential and the effect of the process conditions on the process results.

## 2. MATHEMATICAL MODEL OF POWDER HYDRO CANNON

In the description of internal ballistics of the powder hydro cannon fluid is assumed ideal and incompressible, nozzle profile is smooth, radial flow, heat transfer and atmosphere pressure are insignificant. Quasi-stationary powder combustion is occurs on surface in parallel layers by geometric law and combustion rate depends only on the pressure of powder gases [8], parameters of powder gases are bonded by a simplified Van der Waals equation. Initiation of the powder ignition is assumed to be a process beginning. Point of origin is located at the nozzle entrance.

In this problem the fluid flow is described by the equations

$$\frac{\partial u}{\partial x} = 0, \quad \frac{\partial u}{\partial t} + \frac{\partial}{\partial x} \left( \frac{u^2}{2} + \frac{p}{\rho} \right) = 0 \quad (1)$$

at the initial and boundary conditions

$$u(0, x) = 0, \quad p(0, x) = 0, \quad x_{g0} \leq x \leq x_{f0}; \quad (2)$$

$$p(t, x_f) = 0, \quad p(t, x_g) = p_g, \quad u(t, x_g) = u_g;$$

$$p(t, x_k) = 0, \quad (3)$$

Boundary condition  $p(t, x_k) = 0$  at the end of collimator is applied at the end of collimator when water flows out.

Gunpowder combustion is described by the following system of the ordinary differential equations at the with initial conditions [4, 5, 9]

$$\begin{aligned}
\frac{dz}{dt} &= \frac{u_1}{h_1} p_g; \quad Q_g = m_{p0} \sigma(z) \frac{dz}{dt}; \\
\frac{dV_g}{dt} &= u_g F + \left( \frac{1}{\rho_p} - \alpha \right) Q_g; \quad \frac{dx_g}{dt} = u_g; \\
\frac{dp_g}{dt} &= \frac{1}{V_g} \left[ (k-1) q Q_g - p_g \left( k u_g F + \left( \frac{1}{\rho_p} - \alpha \right) Q_g \right) \right]; \\
z = 0, \quad V_g &= V_{g0}, \quad p_g = p_{g0}, \quad x_g = x_{g0}.
\end{aligned} \tag{4}$$

For an incompressible fluid the partial differential equations (1) can be reduced to a system of the ordinary differential equations. From mass conservation equation in the system (1) it follows, that velocity of any point in the fluid is related to the velocity of the gas-liquid interface by the equation

$$u(t, x) = u_g(t) \frac{F_g(t)}{F(x)}, \tag{5}$$

where subscript ‘‘g’’ designates parameters at the gas-liquid interface. Substituting (5) into momentum equation of the system (1) and, taking into account that  $u_g$  and  $F_g$  depend only on  $t$ , and  $F$  – on  $x$ , the following equation is obtained

$$\dot{u}_g \frac{F_g}{F} + \frac{u_g^2}{F} F'(x_g) + \frac{\partial}{\partial x} \left( \frac{u_g^2 F_g^2}{2F^2} + \frac{p}{\rho} \right) = 0, \tag{6}$$

where  $\dot{u}_g = du_g/dt$ ,  $F'(x_g) = dF/dx$  at  $x = x_g$ . Component  $\frac{u_g^2}{F} F'(x_g)$  appears only for movement of rear interface in nozzle ( $x_g > 0$ ), where the cross section changes along the axis as  $F_g = F(x_g)$ . In this case in any cross section  $x$  velocity will be changing with time even if acceleration of rear interface will be zero ( $\dot{u}_g = 0$ ), due to changing  $F_g$ .

Integration of liquid movement equation (6) from  $x$  to  $x_f$  taking into account boundary condition (2)  $p(t, x_f) = 0$  on the free surface, yields:

$$\left[ \dot{u}_g F_g + u_g^2 F'(x_g) \right] \int_x^{x_f} \frac{d\xi}{F(\xi)} + \frac{u_g^2 F_g^2}{2} \left( \frac{1}{F_f^2} - \frac{1}{F^2(x)} \right) - \frac{p(x)}{\rho} = 0.$$

From the equation above it follows that the pressure distribution and liquid movement equation have the form

$$p(x) = \rho \left[ \left[ \dot{u}_g F_g + u_g^2 F'(x_g) \right] \int_x^{x_f} \frac{d\xi}{F(\xi)} + \frac{u_g^2 F_g^2}{2} \left( \frac{1}{F_f^2} - \frac{1}{F^2(x)} \right) \right], \tag{7}$$

$$\dot{u}_g = \frac{1}{F_g} \left\{ \left[ \frac{p_g}{\rho} - \frac{u_g^2}{2} \left( \frac{F_g^2}{F_k^2} - 1 \right) \right] \left( \int_{x_g}^{x_f} \frac{d\xi}{F(\xi)} \right)^{-1} - u_g^2 F'(x_g) \right\}. \quad (8)$$

The boundary condition at the exit of the collimator are determined by equation (3). The boundary condition determined by equations (2) and (3) are essentially the same, however in (3) the coordinate  $x_k$  is taken as free surface coordinate.

Equations of fluid flow (7) and (8) contain unknown time depending variables such as the powder gases pressure  $p_g$ , coordinate  $x_g$  and velocity  $u_g$  of liquid gas interface, coordinate  $x_f$  of free surface and area  $F_f = F(x_f)$ . Coordinates  $x_f$  and  $x_g$  are related via equation of mass conservation, which for the inflow stage has form

$$\int_{x_g}^{x_f} F(x) dx = F_c L. \quad (9)$$

If nozzle profile is set, then from (9) an algebraic equation is obtained after integration, which relates  $x_f$  and  $x_g$ . However for numerical solution of fluid governing equations it is more convenient to use differential not algebraic relation between coordinates

$$\dot{x}_f = u_g \frac{F_g}{F_f}. \quad (10)$$

Thus, internal ballistics of powder hydro cannon for an ideal incompressible fluid is described by the following system of ordinary differential equations with initial conditions

$$\begin{aligned} \frac{du_g}{dt} &= \frac{1}{F_g} \left\{ \left[ \frac{p_g}{\rho} - \frac{u_g^2}{2} \left( \frac{F_g^2}{F_k^2} - 1 \right) \right] \left( \int_{x_g}^{x_f} \frac{d\xi}{F(\xi)} \right)^{-1} - u_g^2 F'(x_g) \right\} \\ \frac{dx_g}{dt} &= u_g, \quad \frac{dx_f}{dt} = u_g \frac{F_g}{F_f} \\ \frac{dz}{dt} &= \frac{u_1}{h_1} p_g, \quad \frac{dV_g}{dt} = u_g F + \alpha_1 Q_g, \\ \frac{dp_g}{dt} &= \frac{1}{V_g} [(k-1)q Q_g - p_g (ku_g F + \alpha_1 Q_g)]; \end{aligned} \quad (11)$$

$$z = 0, \quad V_g = V_{g0}, \quad p_g = p_{g0}, \quad x_g = x_{g0}, \quad u_g = 0, \quad x_f = x_g + L.$$

Here  $Q_g = m_{p0} \sigma(z) dz/dt$ ,  $\alpha_1 = 1/\rho_p - \alpha$ .

Considering for an example a hydro cannon with a conic nozzle, which cross section radius change according to a law [5]:  $R = kx + b$ , where  $k = (R_s - R_c)/L_s$  and  $b = R_c$ , where  $R_c$ ,  $R_s$  and  $L_s$  – radii of nozzle entrance and exit and nozzle length,  $x_s$  – coordinate of nozzle end.. Then nozzle cross section area change according to the law

$$F = \begin{cases} F_c, & x \leq 0, \\ \pi(kx + b)^2, & 0 \leq x \leq x_s, \\ F_s, & x_s \leq x \leq x_k. \end{cases} \quad (12)$$

Integration of (9) yields, for example, for  $0 \leq x_f \leq x_s$

$$\int_{x_g}^{x_f} F(x) dx = -F_c x_g + \frac{\pi}{3k} [(kx_f + b)^3 - b^3] = F_c L.$$

Then a relation between coordinates  $x_f$  и  $x_g$  at the all stages of the flow development

$$x_f = \begin{cases} x_g + L, & x_g \leq x_{gs}, \\ \frac{1}{k} \left[ \left( \frac{3kF_c}{\pi} (L + x_g) + b^3 \right)^{\frac{1}{3}} - b \right], & x_{gs} \leq x_g \leq x_{gk}, \\ x_s + \frac{1}{F_s} \left[ F_c (L + x_g) - \left( \frac{\pi}{3k} (kL_s + b)^3 - b^3 \right) \right], & x_{gk} \leq x_g \leq 0. \end{cases} \quad (13)$$

Here  $x_{gs} = V_s/F_c - L$  – rear interface coordinate at the moment when water completely fills the nozzle,  $V_s$  – nozzle volume,  $x_{gk} = x_{gs} + V_k$  – coordinate of rear surface at the moment when water fully fills collimator.  $V_k$  – collimator volume. During the fluid exit  $x_f = x_k = const$  and coordinate  $x_f$  does not depend on  $x_g$ .

Thus dynamics of hydro cannon for incompressible fluid is governed by the system of the ordinary differential and algebraic equations (4), (7) and (8) with corresponding initial conditions. This problem can be solved numerically, for example using Runge-Kutta method or more simple Euler method.

### 3. ESTIMATION OF THE EFFECT OF THE FLUID COMPRESSIBILITY

Estimation of fluid compressibility effect on flow parameters can be done as following. The

sonic speed of water can be defined as  $a = \sqrt{\left( \frac{\partial p}{\partial \rho} \right)_s} = \sqrt{\frac{n(p+B)}{\rho}}$ . At the atmospheric pressure

this speed is equal to  $a_0 \approx 1500$  m/s. It is expected that with increase of the sonic speed, that is decrease of the fluid compressibility, solution of the fluid flow problem converges to the solution

for the incompressible fluid flow. Formally this can be done by increasing adiabatic coefficient  $n$  in the state equation in the following way:  $a'_0 = a_0 \sqrt{n'/n}$ . For example for  $n' = 400 n$  sonic speed is  $a'_0 = 20 a_0 = 30 \text{ км/с}$ . If the increase of the sonic speed changes computational results insignificantly, then the fluid compressibility can be disregarded. Otherwise fluid compressibility should be taken into account. The closed form solution available for the incompressible fluid enables us to estimate the accuracy of the computational procedure used for the compressible fluid. If the at increase of the sonic speed solution for the compressible fluid converges to a known solution for incompressible fluid, then the computational procedure is accurate.

Following reasoning could be suggested to corroborate the above considerations. Let us write movement equations of an ideal compressible fluid in the form

$$\frac{d\rho}{dt} + \rho \nabla \bar{u} = 0, \quad \frac{d\bar{u}}{dt} + \frac{1}{\rho} \nabla p = 0. \quad (14)$$

Converting equations by exclusion of derivative of  $\rho$  over time, obtain

$$\frac{1}{a^2} \frac{dp}{dt} + \rho \nabla \bar{u} = 0, \quad \frac{d\bar{u}}{dt} + \frac{1}{\rho} \nabla p = 0. \quad (15)$$

Assume that the velocity and pressure in hydro cannon increase to values  $u$  and  $p$  over time  $t$  on distance  $L$ . Then the items in the above equations can be evaluated as following

$$\frac{1}{a^2} \frac{dp}{dt} \sim \frac{1}{a^2} \frac{p}{t}, \quad \rho \nabla \bar{u} \sim \rho \frac{u}{L}, \quad \frac{d\bar{u}}{dt} \sim \frac{u}{t}, \quad \frac{1}{\rho} \nabla p \sim \frac{p}{\rho L}. \quad (16)$$

Comparison of the order of items in the momentum equation yields

$$\frac{p}{\rho L} = \frac{u}{t}. \quad (17)$$

As the velocity change over time  $t$  on distance  $L$ , then  $u = L/t$  and thus  $p = \rho u^2$ , which conform to the Bernoulli equation by the order of magnitude of parameters. Compare items' order of magnitude in the equation of mass conservation we obtain

$$\frac{1}{a^2} \frac{dp}{dt} : \rho \nabla \bar{u} \sim \frac{1}{a^2} \frac{pL}{t\rho u} = \frac{L^2}{a^2 t^2} = \frac{u^2}{a^2} = M^2. \quad (18)$$

From the equation above follows that the first item in at  $a \gg u$  can be disregarded. Then the equations of motion for low-compressible fluid take the form of

$$\nabla \bar{u} = 0, \quad \frac{d\bar{u}}{dt} + \frac{1}{\rho} \nabla p = 0. \quad (19)$$

The above equation is a standard form of the equation of the incompressible flow. Thus the following three techniques are available for the flow analysis. These techniques include computational solutions of the equations, describing compressible fluid (water). Another solution describes the water flow at condition of the fluid incompressibility. Finally, the solution is obtained for a compressible fluid at a large  $n$ , which is termed low compressibility solution.

#### 4. COMPUTATIONAL RESULTS

Below are presented the estimation of the water velocity and pressure in the powder hydro cannon at the standard water load and powder charge. The figure 2 presents distribution of pressure (curves 1, 3 and 5) and velocity (curves 2, 4 and 6) along cannon axis when the front of the water surface enter collimator ( $x_f = x_s$ ). Curves 1 and 2 represent the computational results for incompressible fluid obtained by equations (5) and (11) while the curves 3 and 4 are numerical solutions for of the compressible fluid flow obtained by the Godunov method. Circles designate solution by Godunov method for low-compressible fluid (sonic speed  $a = 20a_0$ ).

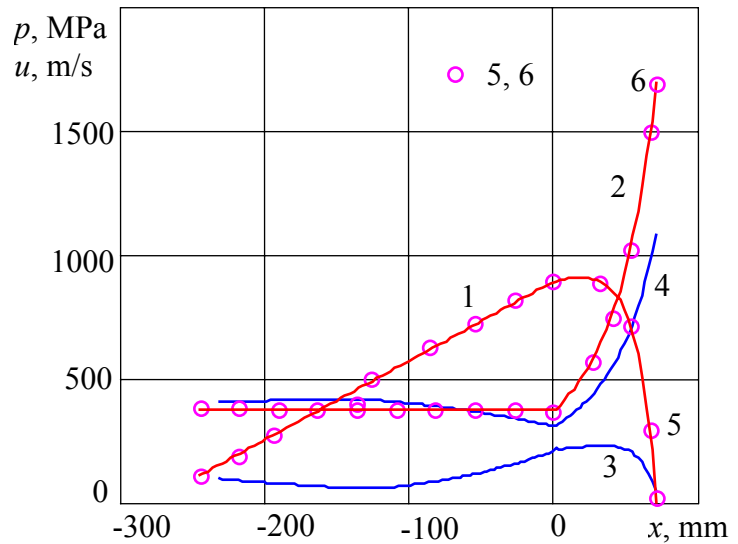


**Figure 2.** Velocity and pressure distribution when front surface reaches collimator for incompressible (1, 2), compressible (3, 4) and low compressible fluid (5, 6). 1, 3 and 5 – pressure; 2, 4 and 6 – velocity.

Charts show that results of calculations for incompressible and compressible

fluids are qualitatively the same, but significantly different quantitatively. The compliance of the velocity curves coincidence is much better than that of the pressure. The results of calculations for the low-compressible and incompressible fluids completely coincide. These facts point that for the considered here hydro cannon compressibility should be taken into account. For compressible fluid maximal pressure equals 240MPa, velocity – 1080m/s. Water density varies less than 10% at such low pressure and should not influence parameters of hydro cannon. Mach number  $M = 0,72$  is also not large. According to the data [10] at these Mach numbers maximal velocity values for incompressible and compressible fluid differ 10%.

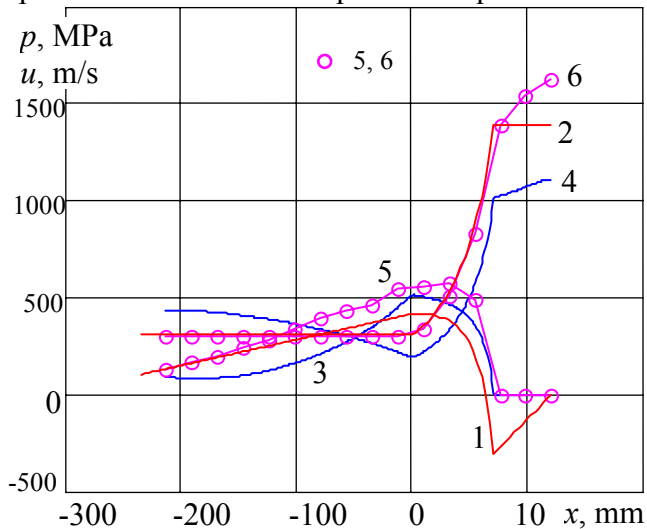


**Figure 3.** Velocity and pressure distribution at the start of the outflow for incompressible (1, 2), compressible (3, 4) and low compressible fluid (5, 6). 1, 3 and 5 – pressure; 2, 4 and 6 – velocity.

Compressibility influence the flow through undulatory processes accompanied by reflection of the waves from front and rear slug surface. Water slug length is about 300 mm in the barrel and characteristic time of wave propagation  $t_x = L/a_0$  is about 0.2ms. Water flows into the nozzle cone of length  $L_s = 70$  with velocity  $u_0 = 400$  m/c. Process duration  $t_p = L_s/u_0 \approx 0,175$  mc is comparable to with characteristic time  $t_x$ . Thus undulatory processes, due to the fluid compressibility will

Compressibility influence the flow through undulatory processes accompanied by reflection of the waves from front and rear slug surface. Water slug length is about 300 mm in the barrel and characteristic time of wave propagation  $t_x = L/a_0$  is about 0.2ms. Water flows into the nozzle cone of length  $L_s = 70$  with velocity  $u_0 = 400$  m/c. Process duration  $t_p = L_s/u_0 \approx 0,175$  mc is comparable to with characteristic time  $t_x$ . Thus undulatory processes, due to the fluid compressibility will

become noticeable in this case. For low-compressible fluid at sonic speed  $a = 20a_0$  characteristic time is  $t_x \approx 0,01mc \ll t_p$  and calculation results coincide with incompressible fluid flow results well. Figure 3 shows distribution of pressure ( curves 1, 3 and 5 ) and velocity ( curves 2, 4 and 6 ) along the cannon axis at the moment of fluid outflow from the nozzle. Incompressible fluid flow is presented by curves 1 and 2, compressible by 3 and 4 and low-compressible by 5 and 6. Coincidence of results at this moment is much better than in the one shown on the figure 1. A nonstationary cavitation occurs in collimator. Negative pressure of about -300MPa on the incompressible fluid chart corresponds to cavitation zone. Cavitation was not taken into account in the incompressible fluid flow, that's why negative pressures are possible. Godunov method used for compressible fluid flow calculation takes cavitation into account and thus there are no negative pressures. Coincidence of calculation results for different fluid models is satisfactory.

Computational results for incompressible and low-compressible fluid are sufficiently close at velocity outside the cavitation zone ( curves 2 and 6 ). In the cavitation zone velocity variation manner differ. Pressure values coincide worse than for velocity in the whole region (curves 1 and 5 ). This difference is explained by the fact that calculations for low-compressible fluid were taking cavitation into account, while calculations for incompressible fluid flow didn't.

## 5. NUMERICAL STUDY OF HYDROCANNON OPERATION

The developed numerical technique was used to examine variation of the water velocity at the exit of the hydro cannon as well as the effect of the design and operational conditions on this velocity. The developed models for incompressible, low compressible and compressible fluids were used for process analysis. It is obvious that while the modeling of the compressible flow brings about the most accurate process evaluation, the use of the incompressible model due to its simplicity makes the process analysis much more practical. Moreover, the closed form solution attainable at the application of the incompressible model enables us to use a rigorous optimization technique for the cannon design. The assumption of the process incompressibility is valid only at the fluid velocity below sonic. Of course, the error resulted from the assumption of the process incompressibility limits such applications, especially at supersonic fluid velocity and, thus, should be evaluated. The performed computations were used for such an evaluation, which show the conditions of the applications of the model in question. The comparison of the computational results obtained at different assumptions (incompressible, low-compressible and compressible) indicates the accuracy of the computations. Indeed, if the procedure is sufficiently accurate, the difference of the water velocities determined by the use of two different models involving low or no compressibility should be insignificant. The performed computations also show the effect of various process variables on the exit water velocity. The most important information which can be obtained as the result of the computations is estimation of the maximal potentially available water velocity as well as the time interval when this velocity is generated.

The charts depicting variation of the exit water velocity and the pressure of combustion products during the water expulsion by the powder combustion products process were constructed for various process conditions and the form of the constructed charts were used for process evaluations. The charts Fig. 4 shows process results at the operational conditions which were maintained in the course of performed experiments. The principal feature of the chart is similarity of the results of co computation for incompressible and low-compressible fluids. Although the numerical techniques are completely different, the computed patterns of the velocity change at both assumptions are almost identical. The maximal velocities in both cases (1,254 m/s for incompressible and 1,450 m/s for low-compressible) attained at the process beginning differ by 196 m/s (almost 14%). However this difference drops as speed of the water drops. At the speed of 1,500 m/s (sound speed in water at room conditions) two patterns became identical, as it is predicted by the analysis of the balance equations. The computed initial value of the velocity of a compressible fluid is 1,050 m/s which is below velocity of the incompressible liquid by 204 m/s. (about 16%). The pattern of the change of the velocity of compressible liquid is also different. In the beginning of the exit the velocity of this fluid is almost constant (1,000 – 1,050 m/s). This plateau is due to the release of the internal energy accumulated in the compressible medium. After release of this energy and its converging in the kinetic energy of the stream, the behavior of the compressible and incompressible fluid becomes very much similar.

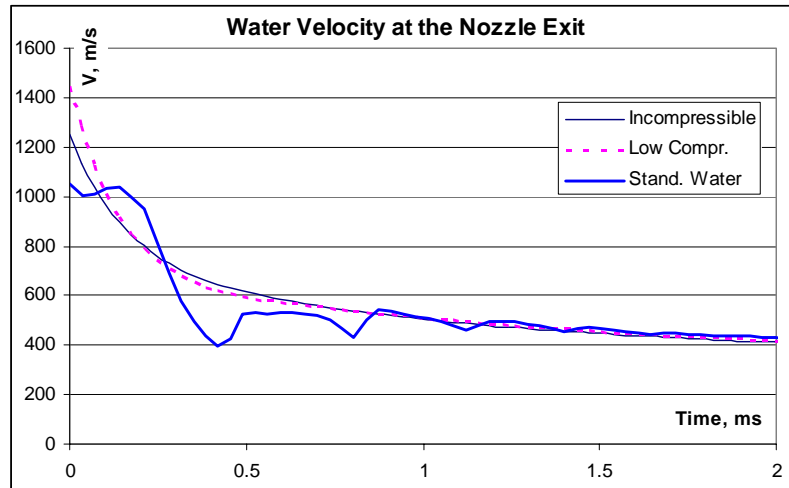


**Figure 4.** Variation of water velocity at the exit of a hydro cannon nozzle for different fluid models.

Process results at various potentially possible conditions were computed in order to determine process peculiarities. The chart Fig. 5 shows the effect of the barrel length on the exit velocity. In this case the length of the barrel was about 8 times more than that used in the experimental device. Due to increase of the momentum exchange between the combustion products and water

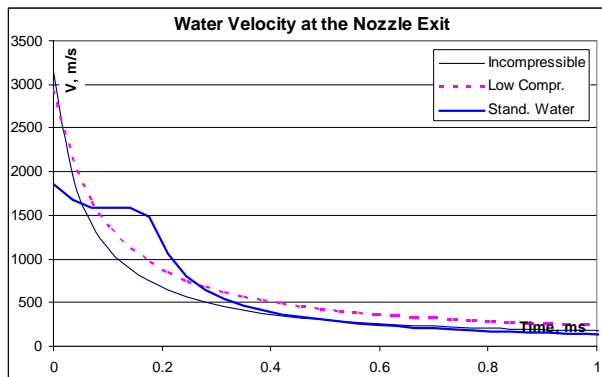


**Figure 5.** Outflow velocity for cannon of 3m barrel length.

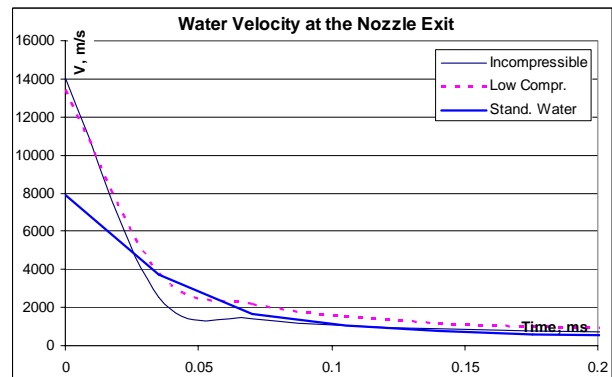


**Figure 6.** Outflow velocity of 115g water load, with 700g powder and 2m barrel.

the water velocity at the beginning of the process reached 1,870 m/s. However the computed pattern of velocity variation does not changed significantly. Significant increase of the water velocity was achieved at the increase of the amount of powder and reduction of the water load. Chart Fig. 6 shows variation of the exit water velocity at the powder mass equal to 700g, the water mass equal to 115g, and the barrel length equal to 2m. At these conditions the water velocity reached 8,000 m/s, while the maximal velocity of the incompressible fluid was 14,000 m/s. There was no velocity plateau in this case and velocity change of both compressible and incompressible fluids have the form of the hyperbola. Increase of the water mass in 4 times changes the velocity pattern dramatically (Fig. 7). The maximal water velocity drops to 3,000 m/s, however more than 50% of the fluid was expelled at the nearly constant (2500 m/s) velocity.

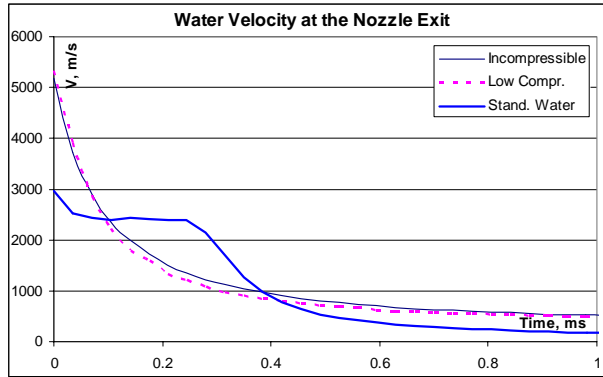


**Figure 7.** Outflow velocity of 460g water load, with 700g powder and 2m barrel.

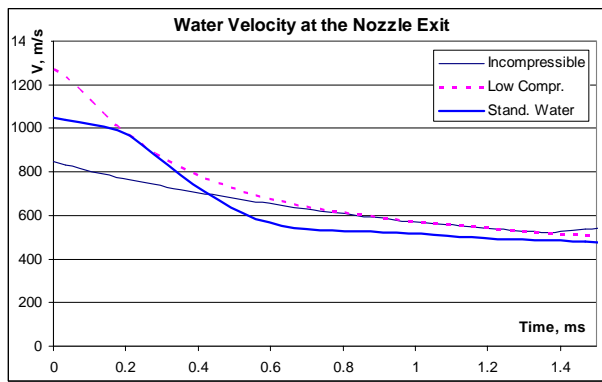


**Figure 8.** Velocity of water outflow from a cannon with long collimator (0.4m)

Dramatic change in the velocity pattern was observed at the increase of the length of the collimator (Fig. 8). In this case the maximal water velocity was only 1,110 m/s. However if at a short collimator significant velocity was maintained only during 0.1-0.2 millisecond and then drops 3-4 times, at a long collimator the exit velocity drops less then 2 times. This change is due to the velocity redistribution along the water stream during the flow through the collimator. In this case, the patterns of the velocities variation of the incompressible and low compressible fluids were substantially different.

Even more dramatic effect on the fluid velocity pattern has the change of the nozzle diameter. At the exit nozzle diameter equal to 0.94 of the barrel diameter (Fig. 9) the velocity of the fluid increases, rather than drops in the course of the exit, while the maximal water velocity attained at the end of the process was only 700 m/s. The patterns of the behavior of the compressible and incompressible fluids were practically the same. Reduction of the nozzle diameter (Fig. 10) brought about the velocity pattern similar to that obtained in previous conditions. The chart Fig. 10 clearly show presence of the wave processes in the course of the exit of the compressible flow.

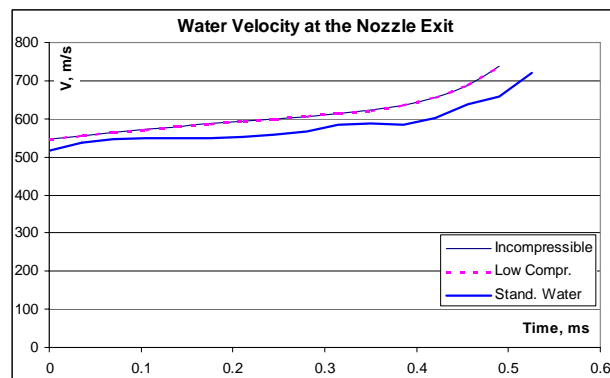


**Figure 9.** Velocity of water outflow from a cannon with nozzle exit 0.94 of barrel dia.

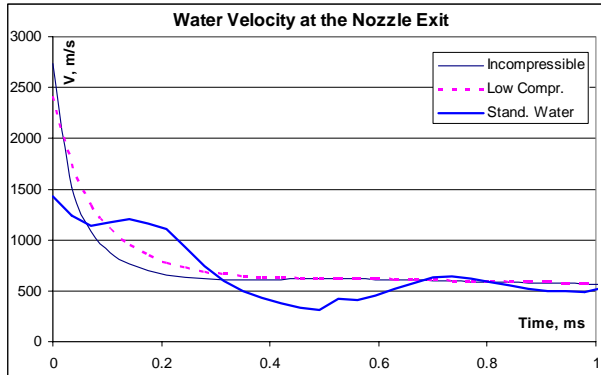


**Figure 10.** Velocity of water outflow from a cannon with nozzle exit 0.34 of barrel dia.

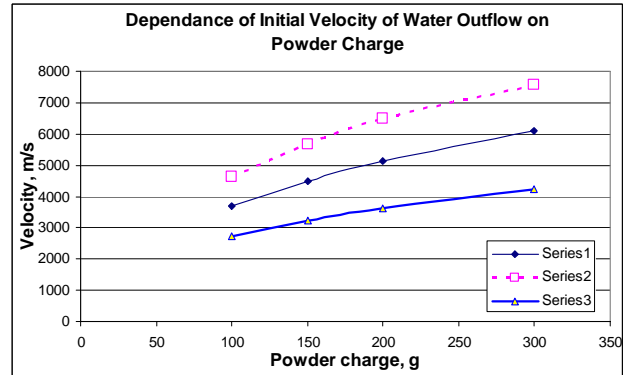


**Figure 11.** Effect of the powder charge mass on initial outflow velocity

The performed computations (totally about 200 cases) enables us to estimate the effect of the various design parameters on the exit velocity. The chart Fig. 11 shows the effect of the powder mass and the chart Fig. 12 shows the effect of the nozzle diameter on the exit water velocity. These charts give clear qualitative correlation between process output and process parameters. It should be noted that while velocity magnitude is quite different, the pattern of the constructed relations for the compressible and incompressible fluids are similar.

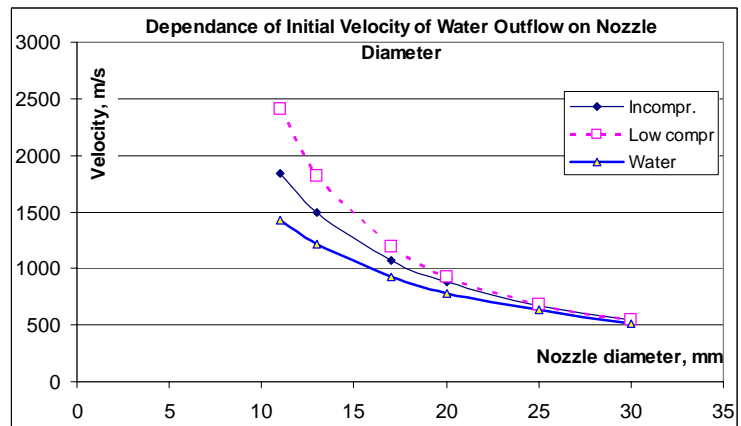


**Figure 12.** Effect of nozzle diameter on initial outflow velocity

Thus, a simplified numerical procedure developed for the incompressible fluid could be used for process design.

## 7. MECHANISM OF FLUID ACCELERATION

Explosion based water acceleration in a hydro cannon is an extremely complicated process, involving multiphase 2D flow of a reacting fluid. It is important from both practical and theoretical considerations to understand the mechanism of momentum transfer from combustion products to the water load. In the barrel of the hydro cannon fluid is accelerated by the expanding combustion products similarly to a solid. The additional fluid acceleration is attained due to wave superposition in a moving fluid, fluid converging in a nozzle and the unsteady radial flow of the fluid in the nozzle. Comparison of the of velocity variation of the compressible and incompressible fluids show that the effect of the wave processes on the on the fluid acceleration is minimal. The fluid compressibility determines accumulation of the internal energy in the fluid, but has minimal effect on the fluid acceleration.

## 6. CONCLUDING REMARKS

The performed computations showed that the fluid compressibility significantly affect flow in the hydro cannon. Calculations for an incompressible fluid yield higher values of pressure and velocity, than those for a compressible one. However, while the numerical values in both cases are different, the process patterns are very much the same. Fluid compressibility in a powder hydro cannon effects the fluid behavior via the undulatory processes, when the duration of these processes is comparable with time of the fluid inflow into the nozzle. Thus estimation of hydro cannon parameters and their optimization can be accomplished using the model of the incompressible fluid, operating with more simple ordinary differential equations rather than much more complicated partial differential equations for compressible fluid.

## 8. ACKNOWLEDGEMENTS

The study was supported by the NSF award DMI-99000247 and CRDF award UE2-2441-DO-02

## 9. NOMENCLATURE

- $t$  – time
- $x$  – coordinate
- $u$  – velocity
- $F$  – area of barrel and nozzle cross section
- $p$  – pressure
- $\rho$  – density
- $n$  and  $B$  – adiabatic coefficient and pressure constant in Teta equation
- $L_s$  and  $L_k$  – nozzle and collimator lengths
- $x_k = L_s + L_k$  – nozzle exit coordinate
- $x_g$  and  $x_f$  – coordinates of water load back and front interface
- $x_{g0}$  and  $x_{f0}$  – initial values of  $x_g$  and  $x_f$
- $p_g$  and  $u_g$  – pressure and velocity of powder gases on water-gas interface.
- $V_g$  – volume of powder gases
- $h_1$  and  $c$  – half of thickness and length of powder grain of tube form
- $u_1$  – combustion coefficient factor
- $z$  – thickness of reacted layer, divided by  $h_1$
- $\sigma(z)$  – relative area of powder combustion depending on the grain form.
- $k$  – adiabatic coefficient of combustion products
- $Q_g$  – rate of powder gases generation
- $\alpha$  – Van der Vaals equation constant, taking into account volume of gas molecules.
- $m_{p0}$  – initial powder mass
- $q$  and  $\rho_p$  – specific heat of combustion and powder density
- $V_{g0}$  and  $p_{g0}$  – gas parameters after primer discharge.

## 10. REFERENCES

1. Atanov G. A. Hydro-impulsive devices for rock breaking, Kiev, 1987, 155p.
2. Voitsehovskiy, B.V., Dudin, Y.A., Nikolaev, Y.A., Nikolaev, V.P., Nikitin, V.V., Cavitation effect in exponential jet nozzle // Dynamics of continuum media., – Novosibirsk: IGD SO AN USSR, 1971, No. 9, pp. 7 – 11
3. Ryhming, J.L. Analysis of unsteady incompressible jet nozzle flow // J. of Appl. Mathematics and Physics (ZAMP). - 1973. - V. 24. P. 149 – 164.
4. Atanov, G., Gubsky, V., Semko, A. The Pressure Rise Factor For Powder Hydro-cannon.- Proceeding of the 13 th International Conference on Jetting Technology. Sardinia, Italy: October 29-31. 1996. pp. 91-103.
5. Atanov G. A., Gubskiy, V.I., Semko, A.N. Internal ballistics of powder hydrocannon // Izv. RAN. Mechanics of liquid and gas., 1977, No.6, pp. 175–179
6. Atanov, G.A., Semko, A.N. Mechanics of the powder hydro-cannon with the regard of wave processes while powder burning // Proceeding of the 9th American Water Jet Conference.- August, 23-26,1997: Dearborn, Michigan.- Paper No 30, pp. 431-440.
7. Godunov, S.K., Zabrodin, A.V., Ivanov, M.Y., Kraiko, A.N., Prokopov, G.P. Numerical solution of multidimensional problems of gas dynamics. Moscow: Nauka, 1976.
8. Design of rocked and barrel systems / edition by B.V. Orlov, Moscow, 1974, 382 p.
9. Atanov, G.A., Semko, A.N. The powder hydro-cannon // Proceedings of International Summer Scientific School “High Speed Hydrodynamics” (HSH 2002).- Cheboksary, Russian/Washington, USA: Cheboksary, Russian, June 16 – 23, 2002. C. 419 – 424.
10. Semko A.N., On effect of fluid compressibility on parameters of hydro-cannon // Engineering and physical journal., 2001, vol. 74, No. 1, pp. 1 – 5.